Original Research
Nada RH. *Glob. South Health Horiz.* 2026 2(3):60-71
10.63950/gshh.2026.2.3.63

Comparative Evaluation of Haematoxylin-Eosin and Masson's Trichrome Staining, with Non-Invasive Indices (FIB-4 and APRI), for Staging Liver Fibrosis: A Blinded Dual-Reader Biopsy Study in Iraq

Stains and Non-Invasive Scores in Liver Fibrosis Staging

NadaRH[1]
1Department of Biology, College of Science, University of Tikrit, Tikrit, Iraq

Date of Submission: 13th April 2026
Date of Acceptance: 10th October 2026
Date of Publication: 31st October 2026

Abstract

Introduction: Accurate staging of liver fibrosis informs prognosis and management in chronic liver disease. Whether stain choice affects staging reproducibility, and how simple serum indices complement histology, remain incompletely studied in Iraqi patients.

Methods: In this cross-sectional study, 80 liver biopsies (METAVIR F0, F1–F2, F3, F4; n = 20 each; HBV, HCV, NAFLD, and other aetiologies) were stained with haematoxylin-eosin (H&E) and Masson's trichrome and independently re-staged by two blinded pathologists. FIB-4 and APRI were calculated; diagnostic performance was assessed using receiver operating characteristic analysis and Spearman correlations.

Results: Inter-reader agreement was higher for Masson's trichrome (weighted $\kappa = 0.979$) than for H&E ($\kappa = 0.939$). Agreement with the original diagnostic stage was 93.8–96.2% versus 76.2–87.5%, respectively. FIB-4 and APRI showed acceptable discrimination of advanced fibrosis (≥F3 area under the curve 0.873 and 0.886, respectively), and both indices correlated strongly with histological stage ($\rho \approx 0.71$) and morphometric collagen area ($\rho \approx 0.69$).

Conclusion: Masson's trichrome improved the reproducibility of fibrosis staging compared with H&E, and FIB-4 and APRI performed acceptably as non-invasive adjuncts that complement, rather than replace, histological assessment. These findings require validation in larger, multicentre studies.

Keywords: Liver fibrosis, Liver biopsy, Masson's trichrome, FIB-4, APRI

Copyright © 2026 The Author(s). Published by the Centre for Epidemiology and Clinical Research. This is an Open Access article under the CC BY 4.0 license.

Introduction

Chronic liver disease is a major cause of morbidity and mortality worldwide, responsible for about two million deaths each year, and is on the rise due to the increased prevalence of viral hepatitis and metabolic dysfunction-associated steatotic liver disease. Although the cause of the fibrosis is not as important as the amount of fibrosis in the liver, in either case progressive accumulation of extracellular matrix leads to cirrhosis, portal hypertension, hepatic decompensation, and hepatocellular carcinoma. Correct staging of fibrosis is thus at the heart of prognosis, antiviral/metabolic treatment and the intensity of surveillance for varices and HCC.

Although liver biopsy is invasive with sampling variability and inter-observer disagreement, it continues to be accepted as the reference standard for assessing liver fibrosis. The METAVIR score is a semi-quantitative score that originally was developed for the clinical evaluation of chronic hepatitis C, and is widely used in other aetiologies, with scores ranging from 0 (absent fibrosis) to 4 (cirrhosis) (1). Fibrosis is typically evaluated on haematoxylin-eosin (H&E) stained sections, but collagen is difficult to appreciate on H&E sections, especially at early and intermediate stages. Special stains like Masson's trichrome allow selective identification of collagen deposition and may enhance visualisation of septa and bridging fibrosis. Recent studies have focused on

Citation: Nada RH. Comparative Evaluation of Haematoxylin-Eosin and Masson's Trichrome Staining, with Non-Invasive Indices (FIB-4 and APRI), for Staging Liver Fibrosis: A Blinded Dual-Reader Biopsy Study in Iraq. Glob. South Health Horiz. 2026 2(3):60-

eISSN: 3093-0014

virtual stain transformation and highlighted the information content of the trichrome stain over the H&E stain in assessing fibrosis in chronic liver disease (2); reproducibility has also been demonstrated to be strongly dependent on the histological platform and scoring system used in Andrew and reliability studies of expanded grading and staging systems (3). The effect of the choice of stain on the reproducibility of the routine METAVIR staging has focused on only a limited extent, however.

Non-invasive tests are becoming more popular because biopsy is impractical to repeat or conduct at the population level. A novel predictor of significant fibrosis and cirrhosis called the aspartate aminotransferase-to-platelet ratio index (APRI) was introduced for use in chronic hepatitis C (4); the fibrosis-4 index (FIB-4) - consisting of aminotransferases, platelets and age - was first validated in HIV/HCV coinfection (5) and subsequently across diverse aetiologies. International guidelines endorse serum-based scores as first-line tools for risk stratification and for ruling out advanced fibrosis in primary care and resource-limited settings, while reserving biopsy or elastography for indeterminate or high-risk cases (6, 7).

In Iraq, chronic liver disease is driven predominantly by chronic hepatitis B and C and, increasingly, by non-alcoholic fatty liver disease (NAFLD). HBV and HCV transmission within screened populations is ongoing in Iraqi Kurdistan, as shown by seroprevalence studies (8) and in diabetes mellitus patients (9). The prevalence rate is also very high for NAFLD; it is very common among Iraqi patients with psoriasis (10). In Basrah, patients with type 2 diabetes had significant liver involvement in the form of fibrosis, as revealed by FibroScan evaluation (11). Data from Iraq also showed that virological/biochemical markers correlate with the histological severity of chronic hepatitis C (12), implementing locally derived non-invasive indices that might contain significant information. However, in Iraq, histopathology services are mostly performed with H&E, and the use of trichrome stains is not consistent, while the performance of FIB-4 and APRI has rarely been validated by histopathology in Iraqi patients.

To our knowledge, no study using biopsies has compared stain-dependent reproducibility of fibrosis staging and diagnostic value of FIB-4 and APRI in a cohort of the same patients. The answer to both questions is clinically meaningful: is it possible to do both at the same time (and improve the agreement between pathologists), and is it possible to have reliable and extensive fibrosis assessment at minimal cost (even if the price of the serum indices is low) in resource-limited settings?

The aim of this study was therefore to compare the reproducibility and agreement with the original diagnostic stage of H&E and Masson's trichrome staining for METAVIR staging of liver fibrosis in a blinded dual-reader re-reading of 80 Iraqi liver biopsies, and to evaluate the diagnostic performance of FIB-4 and APRI, including their correlations with histological stage and morphometric collagen area, for detecting significant fibrosis, advanced fibrosis, and cirrhosis.

Methods

Study Design and Setting

This was a single-centre, cross-sectional study conducted at Tikrit Teaching Hospital, Tikrit, Iraq, over the period from January 2023 to June 2025. The study was designed to compare the inter-stain and inter-reader reproducibility of haematoxylin-eosin (H&E) and Masson's trichrome staining for the histological staging of liver fibrosis, and to evaluate two non-invasive serological indices, the Fibrosis-4 index (FIB-4) and the AST-to-platelet ratio index (APRI), against histological staging as the reference standard.

Study Population

Adult patients (aged 18 years or older) with chronic liver disease attributable to hepatitis B virus (HBV), hepatitis C virus (HCV), non-alcoholic fatty liver disease (NAFLD), or other aetiologies, confirmed serologically and/or clinically, who were scheduled to undergo a diagnostic percutaneous liver biopsy as part of routine clinical care were eligible for inclusion. Patients were excluded if they had a decompensated coagulopathy precluding safe biopsy, a history of liver transplantation, hepatocellular carcinoma, an inadequate biopsy specimen, or if they declined to give consent.

Patients were enrolled during the study period. The last group was divided into four groups of 20 patients each according to the METAVIR fibrosis stage assigned at the first reading of the biopsy: F0 (no fibrosis), F1–F2 (mild-to-moderate fibrosis), F3 (advanced fibrosis) and F4 (cirrhosis). The stratification was done to achieve an equal number of cases with each set of fibrosis severity for the reproducibility analyses.

Clinical Data Collection

At biopsy, the following clinical parameters were recorded for each participant using a structured case report form: sex, age, body mass index (BMI) (weight in kg/height in m2), place of residence, smoking, aetiology of liver disease, duration of disease and history of antiviral treatment or previous liver disease. Each patient underwent a full clinical examination and abdominal ultrasonography, and the presence of jaundice, hepatomegaly, splenomegaly, and ascites was documented. Diabetes mellitus status was also recorded.

Laboratory Assays

Venous blood samples were collected from each patient at the time of biopsy. Serum alanine aminotransferase (ALT), aspartate aminotransferase (AST), alkaline phosphatase (ALP), and gamma-glutamyl transferase (GGT) activities were measured by IFCC-recommended enzymatic methods, and serum albumin was measured by the bromocresol green method, using HUMAN Liquicolor reagent kits (HUMAN

Gesellschaft für Biochemica und Diagnostica, Wiesbaden, Germany). Total bilirubin was measured with reagents from the same manufacturer. All chemistry measurements were performed on a Spinreact Spin XL automated chemistry analyser (Spinreact, Girona, Spain) according to the manufacturer's instructions. Platelet counts were obtained on a Sysmex XN-series automated haematology analyser (Sysmex, Kobe, Japan). The reference ranges used in our laboratory were as follows: ALT and AST up to 40 U/L; ALP 40–130 U/L; GGT 10–60 U/L; total bilirubin 0.3–1.2 mg/dL; albumin 3.5–5.0 g/dL; and platelets 150–400 × 10^3/µL.

Two non-invasive fibrosis indices were calculated from routinely available parameters and required no additional testing. FIB-4 was calculated as (age [years] × AST [U/L])/(platelet count [×10^9/L] × √ALT [U/L]), and APRI was calculated as ((AST/upper limit of normal [40 U/L])/platelet count [×10^9/L]) × 100.

Liver Biopsy and Histopathology

Ultrasound-guided percutaneous liver biopsy was performed using a 16-gauge Tru-Cut needle. Specimens were fixed in 10% neutral buffered formalin, processed routinely, and embedded in paraffin. Sections of 4–5 µm thickness were cut and stained with H&E by the routine protocol. Additional serial sections were stained with Masson's trichrome using the Abcam Masson's Trichrome Stain Kit (ab150686; Abcam, Cambridge, UK) and with Picro Sirius Red using the corresponding Abcam kit (ab150681), in each case according to the manufacturer's instructions; Picro Sirius Red-stained sections were examined under polarised light.

Fibrosis was staged according to the METAVIR system as follows: F0, no fibrosis; F1, portal fibrosis without septa; F2, portal fibrosis with few septa; F3, numerous septa without cirrhosis; and F4, cirrhosis. The original diagnostic stage for each patient was the consensus stage assigned at the original diagnostic reading, at which both the H&E and Masson's trichrome preparations were evaluated together.

Blinded Re-Reading Protocol

To assess inter-stain and inter-reader reproducibility, all stained slides were subjected to a blinded re-reading. A study coordinator who did not participate as a reader removed the original identifying labels and relabelled the slides with unrelated blinded codes (HE- for H&E slides and MT- for Masson's trichrome slides). Two independent readers (Reader A and Reader B), each blinded to the clinical data, laboratory results, the original pathology report, the corresponding slide stained with the other method, and each other's assessments, reviewed the slides. Each reader first examined all 80 H&E slides and then, after a washout period of at least two weeks, examined all 80 Masson's trichrome slides. For each slide, the reader recorded the METAVIR stage, the confidence of the assessment (graded 1-3), specimen adequacy, and the presence of fibrous septa and regenerative nodules. This design allowed quantification of agreement between stains and between readers using kappa methodology (13, 14). The fixed reading order (all H&E slides first, followed by all Masson's trichrome slides) was employed to minimise the risk of direct comparison between stains for the same specimen; however, this approach may introduce period or recall effects, which is acknowledged as a limitation.

Digital Morphometry

Collagen proportionate area was quantified on Masson's trichrome-stained and Picro Sirius Red-stained sections using ImageJ/Fiji software (National Institutes of Health, Bethesda, MD, USA). For each biopsy, five non-overlapping fields were captured and analysed. The fibrosis area percentage was calculated as the fibrotic area divided by the total tissue area, multiplied by 100.

Statistical Analysis

Statistical analyses were performed using SPSS Statistics version 27 (IBM Corp., Armonk, NY, USA) together with validated scripts. The normality of continuous variables was assessed with the Shapiro-Wilk test. Normally distributed data are presented as mean ± standard deviation (SD) and were compared across groups by one-way analysis of variance (ANOVA); non-normally distributed data are presented as median (interquartile range, IQR) and were compared by the Kruskal-Wallis test with Dunn-Bonferroni post-hoc correction. Categorical variables are presented as counts and percentages and were compared by the chi-square test or Fisher's exact test, as appropriate. Associations between continuous or ordinal variables were evaluated with Spearman's rank correlation.

Diagnostic performance of the non-invasive indices and of collagen proportionate area against the histological reference stage was assessed by receiver operating characteristic (ROC) curve analysis, with the area under the curve (AUC) and 95% confidence intervals estimated using a 2000-sample bootstrap procedure. Optimal cutoff values were identified by the Youden index, and sensitivity, specificity, positive predictive value, and negative predictive value are reported for each cutoff in accordance with the STARD reporting recommendations (15). Because the study cohort was stratified to include equal numbers of patients in each METAVIR group, the prevalence of each fibrosis stage in this sample does not reflect that of an unselected clinical population; predictive values should therefore be interpreted with caution. Inter-stain and inter-reader agreement was quantified as the percentage of exact agreement and by quadratic-weighted Cohen's kappa (13), interpreted according to the criteria of Landis and Koch (14). All tests were two-sided, and a p-value < 0.05 was considered statistically significant.

Results

Baseline Characteristics

Eighty liver biopsies were analysed, 20 in each METAVIR group (F0, F1–F2, F3, and F4). As shown in Table 1, age and

disease duration increased significantly with fibrosis stage (both p < 0.0001), whereas sex, BMI, residence, smoking, aetiology, diabetes mellitus, antiviral treatment, and previous liver disease did not differ among the groups (all p > 0.05). Jaundice (p = 0.0002), hepatomegaly (p = 0.0215), and splenomegaly (p < 0.0001) became more frequent with advancing stage, and ascites was observed only in F4 (45%; p < 0.0001).

Table 1: Baseline demographic and clinical characteristics of the study population by METAVIR fibrosis group (n = 80)

Variable	F0 (n = 20)	F1–F2 (n = 20)	F3 (n = 20)	F4 (n = 20)	Test	P value
Age (years)	35.80 ± 8.66	50.45 ± 11.01	50.85 ± 10.60	53.85 ± 6.95	One-way ANOVA	<0.0001
BMI (kg/m²)	28.82 ± 4.95	28.39 ± 5.20	30.85 ± 3.76	30.29 ± 3.82	One-way ANOVA	0.2606
Disease duration (years)	3.60 (1.03–4.45)	5.50 (3.00–9.22)	8.55 (6.50–12.70)	11.85 (9.88–13.50)	Kruskal–Wallis	<0.0001
Sex					Chi-square	0.2615
Male	9 (45%)	7 (35%)	13 (65%)	11 (55%)		
Female	11 (55%)	13 (65%)	7 (35%)	9 (45%)		
Residence					Chi-square	0.2422
Urban	15 (75%)	18 (90%)	18 (90%)	14 (70%)		
Rural	5 (25%)	2 (10%)	2 (10%)	6 (30%)		
Smoking					Chi-square	0.9730
Yes	7 (35%)	7 (35%)	6 (30%)	6 (30%)		
No	13 (65%)	13 (65%)	14 (70%)	14 (70%)		
Aetiology					Chi-square	0.3592
HBV	5 (25%)	4 (20%)	7 (35%)	9 (45%)		
HCV	5 (25%)	10 (50%)	7 (35%)	8 (40%)		
NAFLD	9 (45%)	4 (20%)	5 (25%)	2 (10%)		
Other	1 (5%)	2 (10%)	1 (5%)	1 (5%)		
Diabetes mellitus					Chi-square	0.9425
Yes	17 (85%)	18 (90%)	18 (90%)	18 (90%)		
No	3 (15%)	2 (10%)	2 (10%)	2 (10%)		
Jaundice					Chi-square	0.0002
Yes	0 (0%)	1 (5%)	4 (20%)	9 (45%)		
No	20 (100%)	19 (95%)	16 (80%)	11 (55%)		
Hepatomegaly					Chi-square	0.0215
Yes	2 (10%)	5 (25%)	8 (40%)	10 (50%)		
No	18 (90%)	15 (75%)	12 (60%)	10 (50%)		
Splenomegaly					Chi-square	<0.0001
Yes	0 (0%)	1 (5%)	6 (30%)	14 (70%)		
No	20 (100%)	19 (95%)	14 (70%)	6 (30%)		
Ascites					Chi-square	<0.0001
Yes	0 (0%)	0 (0%)	0 (0%)	9 (45%)		
No	20 (100%)	20 (100%)	20 (100%)	11 (55%)		

Note. Data are mean ± SD, median (interquartile range), or n (%), as appropriate. P values are from one-way ANOVA (age, BMI), Kruskal-Wallis test (disease duration), or chi-square test (categorical variables). BMI, body mass index; HBV, hepatitis B virus; HCV, hepatitis C virus; NAFLD, non-alcoholic fatty liver disease

Laboratory and Morphometric Findings

AST, ALP, GGT, and total bilirubin rose significantly across the fibrosis groups, whereas albumin and platelet count declined (all p < 0.0001); ALT showed a weaker gradient (p = 0.0031) (Table 2). Median fibrosis area increased from 2.10% in F0 to 27.10% in F4 on Masson's trichrome and from 2.20% to 27.55% on Picro Sirius Red (both p < 0.0001), and the two measurements were strongly correlated (ρ = 0.979, p < 0.001). Platelet count (ρ = −0.785) and albumin (ρ = −0.738) correlated inversely with fibrosis stage (both p < 0.001). Representative histological features of each stage on H&E and Masson's trichrome are shown in Figures 1-6.

Table 2: Laboratory parameters, non-invasive fibrosis indices, and morphometric collagen quantification by METAVIR fibrosis group

Variable	F0 (n = 20)	F1–F2 (n = 20)	F3 (n = 20)	F4 (n = 20)	Test	P value
ALT (U/L)	31.00 (20.00–47.00)	45.50 (32.25–64.25)	57.00 (43.50–69.50)	54.00 (35.25–60.00)	Kruskal–Wallis	0.0031
AST (U/L)	25.50 (21.00–30.50)	40.50 (34.75–46.25)	57.50 (46.75–73.75)	66.00 (33.75–84.25)	Kruskal–Wallis	<0.0001
ALP (U/L)	72.35 ± 21.85	85.50 ± 26.88	105.95 ± 28.31	124.65 ± 34.22	One-way ANOVA	<0.0001

GGT (U/L)	26.50 (22.75–33.75)	45.00 (38.75–64.25)	66.00 (50.50–81.75)	82.50 (69.75–107.75)	Kruskal–Wallis	<0.0001
Total bilirubin (mg/dL)	0.81 (0.65–0.89)	0.74 (0.55–1.02)	1.32 (0.84–1.48)	1.97 (1.38–2.17)	Kruskal–Wallis	<0.0001
Albumin (g/dL)	4.36 ± 0.28	4.17 ± 0.29	3.76 ± 0.38	3.35 ± 0.46	One-way ANOVA	<0.0001
Platelets (×10³/μL)	240.95 ± 43.46	199.55 ± 55.42	156.70 ± 39.00	96.15 ± 22.91	One-way ANOVA	<0.0001
FIB-4	0.68 (0.56–0.89)	1.60 (1.01–1.86)	2.75 (1.85–3.86)	5.86 (2.02–7.60)	Kruskal–Wallis	<0.0001
APRI	0.27 (0.20–0.38)	0.52 (0.39–0.65)	0.86 (0.71–1.31)	1.94 (0.74–2.35)	Kruskal–Wallis	<0.0001
Masson's trichrome fibrosis area (%)	2.10 (1.68–2.62)	5.50 (4.25–6.90)	13.40 (11.40–16.23)	27.10 (23.58–28.35)	Kruskal–Wallis	<0.0001
Picro Sirius Red fibrosis area (%)	2.20 (1.80–2.67)	5.80 (5.57–6.95)	15.75 (14.00–16.90)	27.55 (26.27–28.57)	Kruskal–Wallis	<0.0001

Note. Data are mean ± SD for normally distributed variables (one-way ANOVA) or median (interquartile range) for non-normally distributed variables (Kruskal-Wallis test). Normality was assessed with the Shapiro–Wilk test. ALT, alanine aminotransferase; AST, aspartate aminotransferase; ALP, alkaline phosphatase; GGT, gamma-glutamyl transferase; FIB-4, fibrosis-4 index; APRI, aspartate aminotransferase-to-platelet ratio index; PSR, Picro Sirius Red

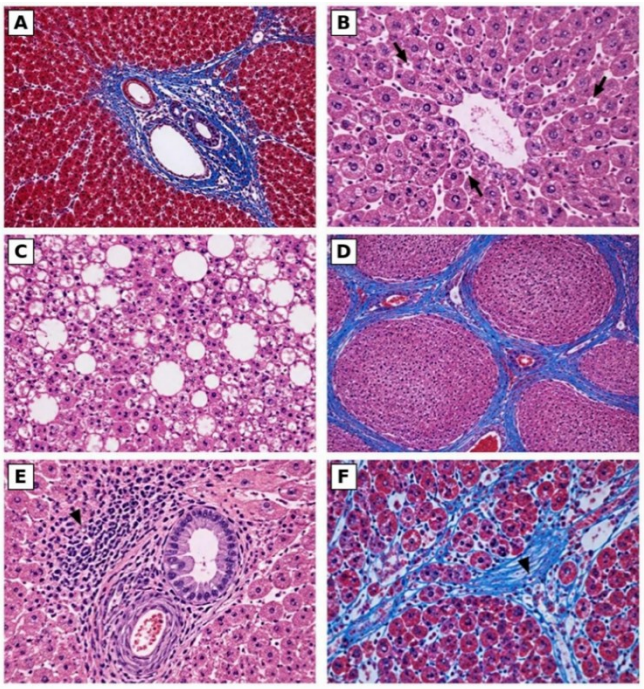


Figure 1: Representative histological features of liver biopsies (H&E and Masson's trichrome)

(A) Masson's trichrome: portal tract with periportal fibrous expansion (collagen blue, hepatocytes red). (B) H&E: preserved lobular architecture around a central vein. (C) H&E: macrovesicular steatosis. (D) Masson's trichrome: regenerative nodules encircled by thick fibrous septa (cirrhosis, METAVIR F4). (E) H&E: portal inflammation with dense lymphocytic infiltrate (arrowhead) adjacent to a bile duct. (F) Masson's trichrome: pericellular collagen deposition (arrowhead). Sample IDs and METAVIR stages: (A) LF-024, F1; (B) LF-007, F0; (C) LF-012, F0; (D) LF-068, F4; (E) LF-031, F2; (F) LF-035, F2. Magnifications/scale bars: (A) ×100, 200 μm; (B) ×400, 50 μm; (C) ×100, 200 μm; (D) ×40, 500 μm; (E) ×400, 50 μm; (F) ×400, 50 μm.

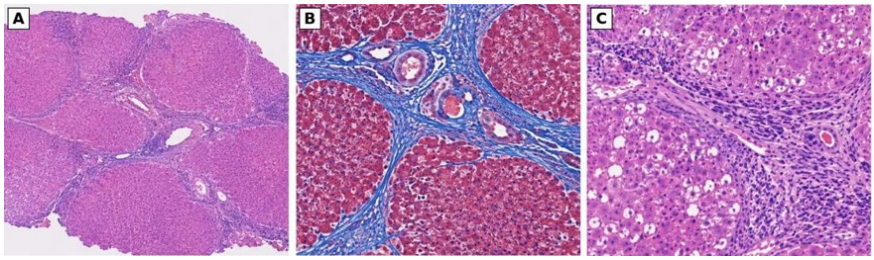


Figure 2: Cirrhotic liver (METAVIR F4): H&E (A, C) and Masson's trichrome (B)

(A) H&E, low power: parenchymal nodules separated by fibrous septa. (B) Masson's trichrome: blue-stained fibrous septa containing vascular and ductular structures. (C) H&E, high power: fibrous septum with inflammatory infiltrate and adjacent steatotic hepatocytes. Sample ID: LF-061. Magnifications/scale bars: (A) ×40, 500 µm; (B) ×100, 200 µm; (C) ×400, 50 µm

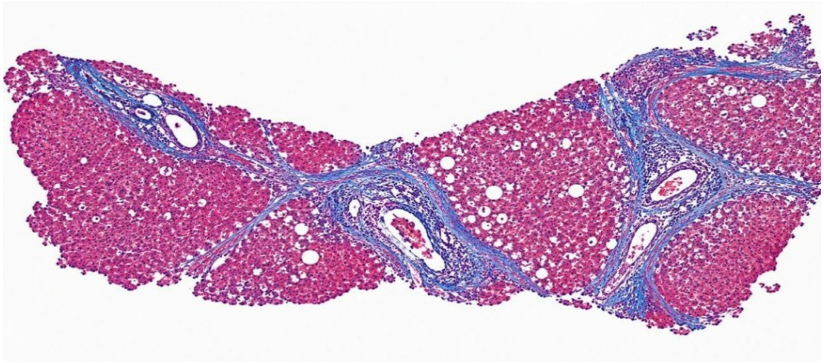


Figure 3: Masson's trichrome-stained liver biopsy core with bridging fibrosis and steatosis

Fibrous expansion of portal tracts with portal-to-portal bridging septa (blue) against red hepatic parenchyma with macrovesicular steatosis. Sample ID: LF-045 (METAVIR F3). Magnification ×40; scale bar = 500 µm

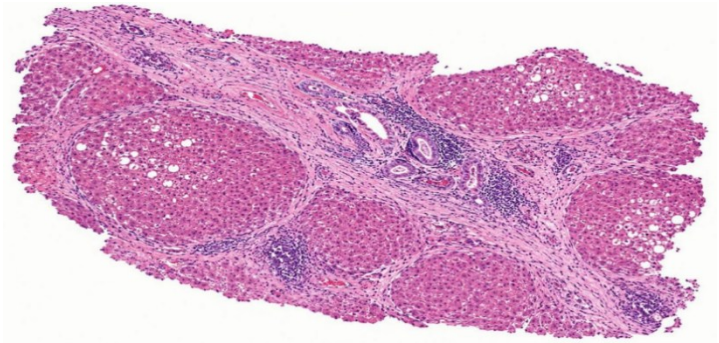


Figure 4: H&E-stained liver biopsy showing established cirrhosis (METAVIR F4)

Nodular architecture with fibrous septa, portal lymphoid aggregates, ductular reaction and mild steatosis. Sample ID: LF-072. Magnification ×40; scale bar = 500 µm

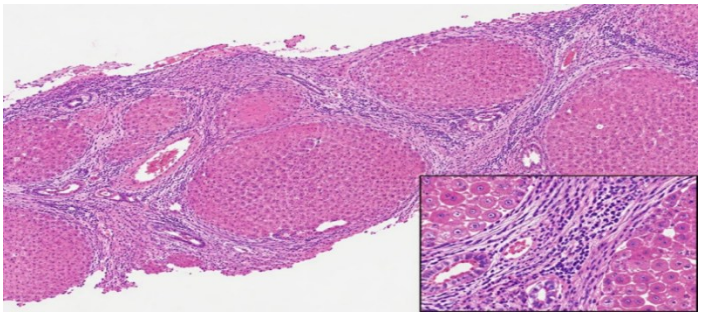


Figure 5: H&E-stained liver biopsy showing parenchymal nodules delineated by fibrous septa

Fibrous septa distort the normal hepatic architecture. Inset: septum with mononuclear inflammatory cells and bile ductules. Sample ID: LF-075 (METAVIR F4). Magnifications: main ×40 (500 µm); inset ×400 (50 µm)

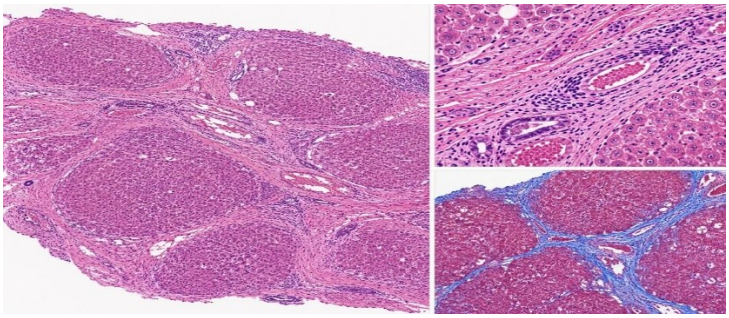


Figure 6: Cirrhotic liver: H&E with corresponding Masson's trichrome detail

H&E, low power, showing regenerative nodules. Insets: H&E detail of a fibrous septum with ductular structures (upper) and Masson's trichrome highlighting septal collagen in blue (lower). Sample ID: LF-079 (METAVIR F4). Magnifications: main ×40 (500 µm); insets ×400 (50 µm)

FIB-4 and APRI across Fibrosis Stages

Median FIB-4 increased from 0.68 in F0 to 5.86 in F4, and median APRI from 0.27 to 1.94 (both $p < 0.0001$; Table 2, Figure 7). On Dunn-Bonferroni post-hoc testing, F0 differed from F3 and F4 for both indices ($p < 0.001$) and F1–F2 differed from F4 (FIB-4, $p = 0.005$; APRI, $p = 0.004$); F0 versus F1–F2 was significant only for FIB-4 ($p = 0.039$), and adjacent advanced stages (F1–F2 vs F3; F3 vs F4) did not differ. Both indices correlated with fibrosis stage ($\rho = 0.706$ and 0.707) and with Masson's trichrome fibrosis area ($\rho = 0.695$ and 0.691; all $p < 0.001$) (Figure 8).

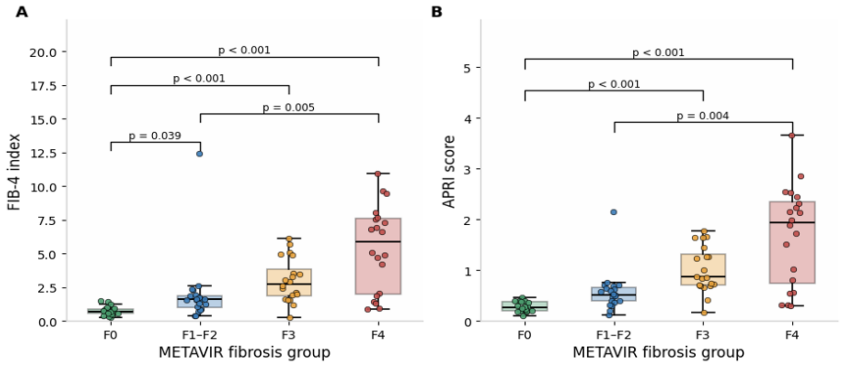


Figure 7: Distribution of FIB-4 (A) and APRI (B) across METAVIR fibrosis groups (n = 20 per group)

Boxes show median and interquartile range; whiskers show range; dots represent individual patients. P values from Dunn's post-hoc test with Bonferroni correction following Kruskal–Wallis (both $p < 0.0001$)

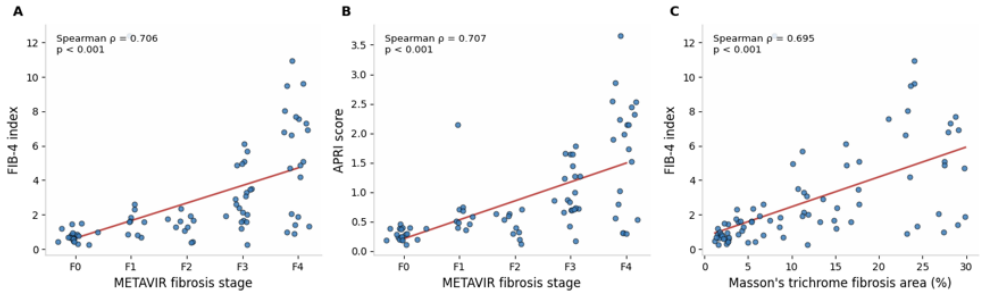


Figure 8: Spearman correlations of FIB-4 (A) and APRI (B) with METAVIR fibrosis stage, and of FIB-4 with the Masson's trichrome fibrosis area percentage (C)

Red line: linear fit shown for visualisation. n = 80

Diagnostic Performance of FIB-4 and APRI

The diagnostic performance of both indices is presented in Table 3 and Figure 9. Accuracy was highest for advanced fibrosis (≥F3), with AUCs of 0.873 for FIB-4 (cutoff 1.89; sensitivity 77.5%, specificity 87.5%) and 0.886 for APRI (cutoff 0.70; sensitivity 80.0%, specificity 90.0%); for significant fibrosis (≥F2), the AUCs were 0.839 and 0.831, respectively. For cirrhosis (F4), both indices showed high specificity (90.0% and 96.7%) but lower sensitivity (70.0% and 60.0%), with AUCs of 0.826 and 0.820. The confidence intervals of the two indices overlapped at all endpoints.

Table 3: Diagnostic performance of FIB-4 and APRI for significant fibrosis (≥F2), advanced fibrosis (≥F3), and cirrhosis (F4)

Index	Endpoint	AUC (95% CI)	Optimal cutoff	Sensitivity %	Specificity %	PPV %	NPV %
FIB-4	Significant fibrosis (≥F2)	0.839 (0.737–0.927)	1.65	72.0	86.7	94.7	50.0
FIB-4	Advanced fibrosis (≥F3)	0.873 (0.785–0.947)	1.89	77.5	87.5	86.1	79.5
FIB-4	Cirrhosis (F4)	0.826 (0.709–0.927)	4.19	70.0	90.0	70.0	90.0
APRI	Significant fibrosis (≥F2)	0.831 (0.733–0.915)	0.53	80.0	83.3	92.3	62.5
APRI	Advanced fibrosis (≥F3)	0.886 (0.801–0.954)	0.70	80.0	90.0	88.9	81.8
APRI	Cirrhosis (F4)	0.820 (0.690–0.931)	1.73	60.0	96.7	85.7	87.9

Note. AUC, area under the receiver operating characteristic curve; CI, confidence interval (bootstrap, 2000 resamples); PPV, positive predictive value; NPV, negative predictive value. Optimal cutoffs were derived from the Youden index. Significant fibrosis, METAVIR ≥F2; advanced fibrosis, ≥F3; cirrhosis, F4. Because the study cohort was stratified to include equal numbers of patients in each METAVIR group, the prevalence of each fibrosis stage in this sample does not reflect that of an unselected clinical population; predictive values should be interpreted with caution

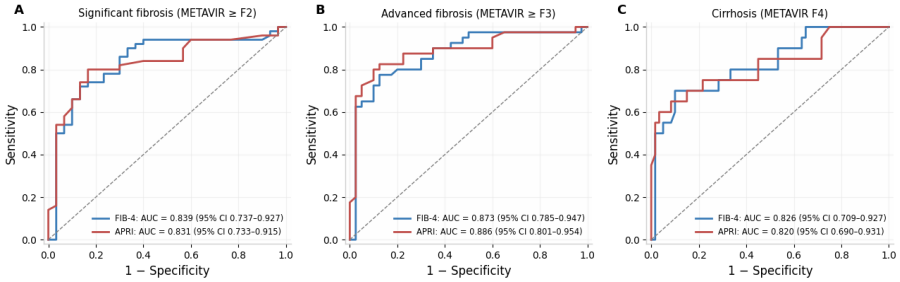


Figure 9: Receiver operating characteristic curves of FIB-4 and APRI for significant fibrosis (A, METAVIR ≥F2), advanced fibrosis (B, ≥F3), and cirrhosis (C, F4)

AUC with 95% confidence intervals (bootstrap, 2000 resamples) is shown for each index.

Inter-Stain and Inter-Reader Agreement

Specimen adequacy was high in all four reading sets (78-79 of 80 biopsies). Inter-stain agreement between H&E and Masson's trichrome was almost perfect for both readers (weighted κ = 0.966 for Reader A and 0.941 for Reader B), with exact agreement of 83.8% and 72.5%, respectively, and all discordances within one stage (Table 4, Figure 10).

Table 4: Inter-stain agreement (H&E versus Masson's trichrome) for blinded METAVIR staging, by reader

Comparison	Reader	n	Exact agreement, %	Within one stage, %	Unweighted κ	Weighted κ
H&E vs Masson's trichrome	Reader A	80	83.8	100.0	0.794	0.966
H&E vs Masson's trichrome	Reader B	80	72.5	100.0	0.656	0.941

Note. Cohen's kappa with quadratic weights was used because METAVIR stages are ordinal. Weighted κ values were interpreted according to Landis and Koch (0.81–1.00, almost perfect agreement). All inter-stain discordances were within one METAVIR stage

Inter-reader agreement was higher on Masson's trichrome (exact agreement 90.0%; weighted κ = 0.979) than on H&E (78.8%; κ = 0.939) (Table 5, Figure 10). Agreement with the original diagnostic METAVIR stage was also higher on Masson's trichrome than on H&E for both Reader A (96.2% vs 87.5%) and Reader B (93.8% vs 76.2%) (Table 5, Figure 11). It should be noted that the original diagnostic stage was itself assigned with knowledge of both stains, which may inflate agreement estimates relative to a truly independent reference standard; these results should therefore be interpreted as measures of agreement rather than as independent diagnostic accuracy.

Table 5: Inter-reader agreement and agreement with the original diagnostic METAVIR stage, by stain

Comparison	Stain	n	Exact agreement, %	Within one stage, %	Unweighted κ	Weighted κ	Agreement with original stage, %
Reader A vs B	H&E	80	78.8	97.5	0.732	0.939	87.5 (A) / 76.2 (B)
Reader A vs B	Masson's trichrome	80	90.0	100.0	0.873	0.979	96.2 (A) / 93.8 (B)

Note. Cohen's kappa with quadratic weights. Agreement with the original diagnostic stage denotes exact agreement between each blinded reading and the METAVIR stage assigned at the original diagnostic assessment. Interpretation of κ per Landis and Koch

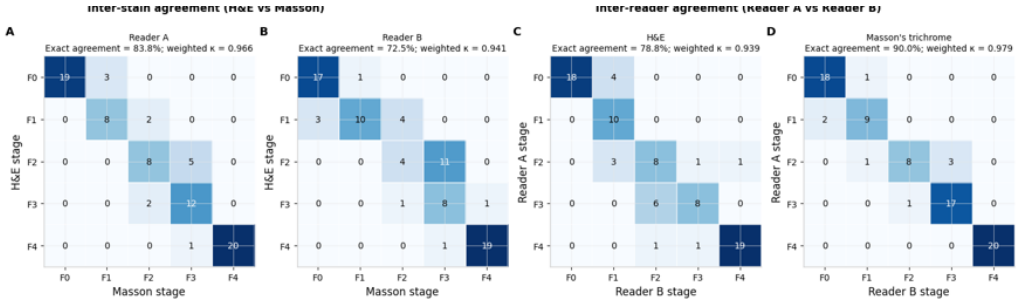


Figure 10: Agreement heat maps for METAVIR staging

(A, B) Inter-stain agreement (H&E rows vs Masson's trichrome columns) for Reader A and Reader B. (C, D) Inter-reader agreement (Reader A rows vs Reader B columns) for H&E and Masson's trichrome. Numbers in cells are biopsy counts

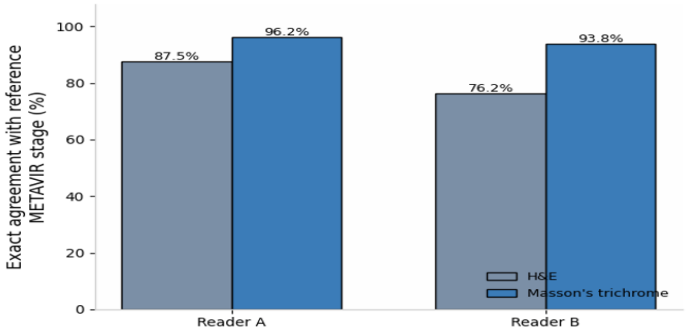


Figure 11: Exact agreement of each stain with the original diagnostic METAVIR stage, by reader
Masson's trichrome showed higher agreement than H&E for both readers

Discussion

In this biopsy-based, cross-sectional study of 80 Iraqi patients spanning the full spectrum of fibrosis severity, we set out to determine whether collagen-selective staining improves the reproducibility of histological staging, and how the widely used serum indices FIB-4 and APRI perform against a histological reference in this population. Three principal findings emerge. First, Masson's trichrome yielded higher inter-reader reproducibility than routine haematoxylin and eosin (H&E), with near-perfect agreement (weighted κ = 0.979 versus 0.939) and consistently better agreement with the original diagnostic METAVIR stage; all inter-stain discordances were confined to a single stage. Second, FIB-4 and APRI rose stepwise with fibrosis stage and showed good overall discrimination for significant and advanced fibrosis (AUCs approximately 0.82–0.89), but their sensitivity for cirrhosis was limited (60–70%) despite high specificity. Third, morphometric collagen quantification on Masson's trichrome and Picro Sirius Red was almost perfectly correlated with each other (ρ = 0.979), and very strongly correlated with fibrosis stage, further supporting the biological plausibility of both the stain comparison and serological trends. In conclusion, this study indicates that a collagen-specific stain would be a valuable addition to the H&E stains used in the histopathological assessment of chronic liver disease and that simple laboratory parameters should only be used as a screening tool and not as a substitute for liver histopathology in this context.

Why Masson's Trichrome Improves Staging Reproducibility

It is easy to understand the superior reproducibility of Masson's trichrome. Aniline blue stains the fibrous material, specifically collagen fibres, and it is the presence or absence of fibrous material that makes the thin septa, early bridging, and early regenerative nodules distinguishable from the hepatocellular background; Thin septa and early bridging can be difficult to identify on H&E in cores with hepatocellular fragmentation or steatosis. Our discordance pattern supports this interpretation: the disagreements between stains and between readers were almost invariably cases in which H&E was called one stage lower than the Masson-based or original diagnostic assignment, consistent with under-recognition of delicate bridging rather than over-reading. This matters most at the intermediate stages (F2-F3), where the presence or absence of bridging determines the stage and, in many aetiologies, the threshold for antiviral treatment or surveillance. The rise in inter-reader exact agreement from 78.8% on H&E to 90.0% on Masson's trichrome is clinically meaningful, because staging systems such as METAVIR were themselves developed with recognition that observer agreement is imperfect (1). Our findings align with reliability studies of expanded NASH staging systems, which report that fibrosis staging benefits from standardised ancillary stains (3). The digital pathology literature provides convergent support: conditional generative adversarial networks can detect and quantify fibrosis on H&E whole-slide images that is poorly visible to the unaided eye (16), and a framework for virtual H&E-to-Masson stain transformation has been proposed precisely because collagen-selective information carries diagnostic value that H&E does not capture (2). Finally, the very strong correlation between morphometric collagen area and stage, and between the two collagen stains (ρ = 0.979), echoes the collagen proportionate area literature, in which quantitative collagen measurement predicts clinically relevant outcomes (17). Masson's trichrome, in short, does not create information but reveals it.

Performance of FIB-4 and APRI in an International Context

Both indices increased monotonically across stages, with Spearman correlations of approximately 0.71 with stage and with morphometric collagen area, confirming that these inexpensive scores capture a genuine biological gradient. Our AUCs (FIB-4: 0.839, 0.873, and 0.826 for ≥F2, ≥F3, and F4; APRI: 0.831, 0.886, and 0.820) sit within the range reported internationally. In an Iranian NAFLD cohort, Amemia and colleagues reported AUROCs of 0.913 for FIB-4 and 0.923 for APRI against FibroScan for advanced fibrosis (18), somewhat higher than ours, plausibly because elastography rather than biopsy was the comparator and the cohort was aetiologically homogeneous. In an Italian chronic hepatitis C cohort, Catanzaro and colleagues reported an AUC of 0.855 for FIB-4 and 0.767 for APRI for cirrhosis (19); our F4 results (0.826 and 0.820) are comparable and, interestingly, show the reverse ordering for APRI, underscoring that the relative performance of the two scores

is cohort-dependent. Chen and colleagues in China reported a FIB-4 AUC of 0.895 for F3–F4 fibrosis (20), and multicentre work in chronic hepatitis B continues to validate FIB-4-derived indices across thresholds (21). Our results are also consistent with the original derivation studies: Wai et al. developed APRI in chronic hepatitis C to predict significant fibrosis and cirrhosis (44), Sterling et al. developed FIB-4 in HIV/HCV coinfection (5), and Vallet-Pichard et al. confirmed its accuracy in HCV against biopsy (22).

These indices have strengths and weaknesses, which can be understood in terms of their pathophysiology. Platelet count was most strongly associated with stage in our cohort ($\rho = -0.785$), and this was typical of portal hypertension, as evidenced by hypersplenic sequestration and decreased production of thrombopoietin in the liver. AST increases with increasing hepatocellular damage and decreasing clearance. The age term in FIB-4 also played a significant role here: people in our F0 group were significantly younger (mean 35.8 years), so their scores were correspondingly lower, and the separation was better, but this could mean that performance looked better than it would have in age-matched comparisons. On the other hand, the low sensitivity of the two tests (for cirrhosis: FIB-4 70%, APRI 60%) is biologically plausible: patients with burnt-out compensated cirrhosis can have near-normal aminotransferases and be below the cut-off, whereas transient AST flares can spuriously raise APRI in patients with minimal fibrosis.

Comparison with Iraqi Studies

To date, few studies have directly compared histological staining of fibrosis staging in biopsy specimens in Iraq, and our study fills this gap. Prior Iraqi studies have mostly used non-invasive modalities. Abdullah and co-researchers utilised FibroScan to gauge liver involvement among type 2 diabetic patients in Basrah and linked stiffness to metabolic danger factors (11) in a case-control study, and Dhaher and colleagues studied NAFLD in patients with psoriasis in Iraq (10). FIB-4 has been calculated in an Iraqi NAFLD cohort by Alzubaidi and colleagues in the context of microRNA biomarker evaluation (23), and Esmail and colleagues reported improvements in liver fibrosis scores following short-term orlistat therapy in Iraqi patients with NAFLD and metabolic syndrome (24). Beyond fibrosis indices per se, Al-Nimer applied the albumin-bilirubin (ALBI) score, supported by haematological indices, in Iraqi patients with non-malignant liver disease (25), and Abbas evaluated alpha-fetoprotein and high-sensitivity C-reactive protein in Iraqi patients with liver cirrhosis (26). Histology-correlative Iraqi work is scarce: Al-Khurri and colleagues correlated serum HCV RNA with histological features in chronic hepatitis C (12) but did not address staining methodology or staging reproducibility. Our biopsy-based, dual-stain, dual-reader design therefore complements this predominantly elastography- and serology-based national literature, and suggests that the FIB-4 and APRI performance reported in Iraqi cohorts is consistent with biopsy-anchored data from the same population.

Clinical Implications

Based on our data, there are two pragmatic steps that we want to take. In fact, histology is the reference standard, and in histology, H&E alone was adequate at the extremes (F0 and unequivocal F4); however, Masson's trichrome is very useful at the intermediate F2–F3 stage where most of our differences arose, and we suggest it should be used routinely in staging biopsies of chronic liver disease. In resource-limited settings in Iraq, FIB-4 and APRI are useful triage tools that can be performed using only routine laboratory parameters, and their negative predictive values suggest their use as rule-out rather than definitive diagnostic tools, in line with international guidelines which place serum scores as first-line, rule-out tests (6, 7). With the low cirrhosis sensitivity, a low score should not be used to rule out cirrhosis, and a serological triage with histology use in indeterminate cases seems most defensible.

Study Limitations

There are a few caveats to interpretation. Our AUCs and κ estimates are slightly imprecise due to the small number of cases (n = 80; 20 per group) and single-centre design of this study. Prognostic performance cannot be evaluated in a cross-sectional design. The cohort was stratified to have an equal number of patients in each METAVIR group, and the prevalence of fibrosis stages in an unselected clinical population is different, influencing the interpretability of the predictive values and possibly overestimating the apparent diagnostic performance. The original diagnostic METAVIR stage was derived from the study slides (although by a different consensus exercise, which did include stains), and this may overestimate the estimates of agreement when compared to a truly independent reference standard; this was not eliminated in the design, though we did attempt to minimise it by blinding and washout. The fixed reading order (all H&E slides first, followed by all Masson's trichrome slides) may have introduced period or recall effects. Aetiologies were pooled (HBV, HCV, NAFLD, and other), and index cut-offs are known to be aetiology-dependent, so our thresholds should not be generalised to single-aetiology populations. We did not include a transient elastography comparison, and both readers were from one institution, so inter-institutional generalisability of the reproducibility estimates is untested. Finally, the morphometry protocol did not include formal blinding of the morphometrist or assessment of repeat-measurement reliability, which may introduce measurement bias.

Future Directions

Multicentre Iraqi validation, with readers and biopsies from several institutions, is the most immediate priority. Digital pathology and AI-assisted fibrosis quantification, including virtual H&E-to-Masson stain transformation (2) and GAN-

based fibrosis detection on H&E (16), could deliver the reproducibility benefits of collagen-selective staining without additional histochemical workload, and merit prospective evaluation against our morphometric benchmark. The use of serum indices, the establishment of aetiology-specific cut-off levels, and prospective studies linking the serum-based staging with clinical outcomes using elastography and collagen proportionate area (17) would add to the translation to the picture.

Conclusion

In this biopsy-based cross-sectional study of 80 Iraqi patients, Masson's trichrome staining yielded higher inter-reader reproducibility and closer agreement with the original diagnostic METAVIR stage than haematoxylin-eosin, with all inter-stain discordances confined to a single stage. FIB-4 and APRI showed acceptable discrimination of significant fibrosis, advanced fibrosis, and cirrhosis, and both correlated strongly with histological stage and with morphometric collagen area. These findings suggest that routine use of Masson's trichrome can improve the reliability of fibrosis staging where it is not already standard practice, and that FIB-4 and APRI are useful, inexpensive adjuncts for risk stratification in resource-limited settings. Neither serum index should replace histology; rather, non-invasive scores and optimised staining are complementary components of fibrosis assessment. Larger, prospective, multicentre studies across aetiologies are warranted to confirm these findings.

Abbreviations

ALP: alkaline phosphatase
ALT: alanine aminotransferase
ANOVA: analysis of variance
APRI: aspartate aminotransferase-to-platelet ratio index
AST: aspartate aminotransferase
AUC: area under the receiver operating characteristic curve
BMI: body mass index
CI: confidence interval
FIB-4: fibrosis-4 index
GGT: gamma-glutamyl transferase
H&E: haematoxylin-eosin
HBV: hepatitis B virus
HCV: hepatitis C virus
IQR: interquartile range
METAVIR: Meta-analysis of Histological Data in Viral Hepatitis
NAFLD: non-alcoholic fatty liver disease
NPV: negative predictive value
PPV: positive predictive value
PSR: Picro Sirius Red
ROC: receiver operating characteristic
SD: standard deviation
STARD: Standards for Reporting of Diagnostic Accuracy Studies.

Declarations

Ethics Approval and Consent to Participate: The study protocol was approved by the Institutional Ethics Committee of the University of Tikrit (approval No. TU-IAEC-2024-037). The study was conducted in accordance with the Declaration of Helsinki, and written informed consent was obtained from all participants.

Data Availability: The datasets generated and analysed during the current study are available from the corresponding author on reasonable request.

Competing Interests: The author declares that she has no competing interests.

Funding sources: This research received no specific grant from any funding agency in the public, commercial, or not-for-profit sectors.

Author contributions: NRH: Conceptualisation, Methodology, Investigation, Formal analysis, Writing – original draft preparation, Writing – review and editing, Visualisation. The author read and approved the final manuscript.

Acknowledgements: The author thanks the laboratory and pathology staff of Tikrit Teaching Hospital, Tikrit, Iraq, for their technical assistance.

References

1. Bedossa P, Poynard T; METAVIR Cooperative Study Group. An algorithm for the grading of activity in chronic hepatitis C. Hepatology. 1996;24(2):289-293. https://doi.org/10.1002/hep.510240201
2. Balaha HM, Ali KM, Mahmoud A, Aboudessouki A, Azam MT. From haematoxylin and eosin to Masson's trichrome: a comprehensive framework for virtual stain transformation in chronic liver disease diagnosis. Diagnostics (Basel). 2026;16(5):764. https://doi.org/10.3390/diagnostics16050764
3. Loh Jiezhen T, Salomao M, Moreira R, Pai R. Reliability of an expanded non-alcoholic steatohepatitis grading and staging system for assessment of disease activity and fibrosis. Int J Surg Pathol. 2025;33(2):281-288. https://doi.org/10.1177/10668969241260226
4. Wai CT, Greenson JK, Fontana RJ, Kalbfleisch JD, Marrero JA, Conjeevaram HS, et al. A simple noninvasive index can predict both significant fibrosis and cirrhosis in patients with chronic hepatitis C. Hepatology. 2003;38(2):518-526. https://doi.org/10.1053/jhep.2003.50346
5. Sterling RK, Lissen E, Clumeck N, Sola R, Correa MC, Montaner J, et al. Development of a simple noninvasive index to predict significant fibrosis in patients with HIV/HCV coinfection. Hepatology. 2006;43(6):1317-1325. https://doi.org/10.1002/hep.21178
6. European Association for the Study of the Liver. EASL Clinical Practice Guidelines on non-invasive tests for evaluation of liver disease severity and prognosis - 2021 update. J Hepatol. 2021;75(3):659-689. https://doi.org/10.1016/j.jhep.2021.05.025

7. Sterling RK, Duarte-Rojo A, Patel K, Asrani SK, Alsawas M, et al. AASLD Practice Guideline on imaging-based noninvasive liver disease assessment of hepatic fibrosis and steatosis. Hepatology. 2025;81(2):672-724. https://doi.org/10.1097/HEP.0000000000000843
8. Naqid IA, Mahmood AJ, Mosa AA, Ahmed ZS, Abdullah AS. Hepatitis B and C virus infection among couples undergoing premarital screening in Iraqi Kurdistan. IJID Reg. 2025;14:100492. https://doi.org/10.1016/j.ijregi.2024.100492
9. Merza MA. Seroprevalence and risk factors of hepatitis B and C viruses among diabetes mellitus patients in Duhok province, Iraqi Kurdistan. J Family Med Prim Care. 2020;9(2):642-646. https://doi.org/10.4103/jfmpc.jfmpc_1158_19
10. Dhaher SA, Hilfi NZ, Abdullah MA. Non-alcoholic fatty liver disease among Iraqi patients with psoriasis: a case-control study. Cureus. 2024;16(4):e57487. https://doi.org/10.7759/cureus.57487
11. Abdullah MA, Kadhum FJ, Issa SS. Assessment of liver involvement in patients with type 2 diabetes mellitus in Basrah City, Iraq, using FibroScan and correlation with risk factors. Cureus. 2024;16(7):e65089. https://doi.org/10.7759/cureus.65089
12. Al-Khurri LE, Al-Khafaji KR, Al-Salihi SA, Alwaysi SA. Serum HCV-RNA levels in patients with chronic hepatitis C: correlation with histological features. Arab J Gastroenterol. 2009;10(1):10-13. https://doi.org/10.1016/j.ajg.2009.03.003
13. Cohen J. Weighted kappa: nominal scale agreement with provision for scaled disagreement or partial credit. Psychol Bull. 1968;70(4):213-220. https://doi.org/10.1037/h0026256
14. Landis JR, Koch GG. The measurement of observer agreement for categorical data. Biometrics. 1977;33(1):159-174. https://doi.org/10.2307/2529310
15. Bossuyt PM, Reitsma JB, Bruns DE, Gatsonis CA, Glasziou PP, Irwig L, et al. STARD 2015: an updated list of essential items for reporting diagnostic accuracy studies. BMJ. 2015;351:h5527. https://doi.org/10.1136/bmj.h5527
16. Naglah A, Khalifa F, El-Baz A, Gondim D, et al. Conditional GAN-based system for fibrosis detection and quantification in Hematoxylin and Eosin whole slide images. Med Image Anal. 2022;81:102537. https://doi.org/10.1016/j.media.2022.102537
17. Israelsen M, Guerrero Misas M, Koutsoumourakis A, Huang Y, Thiele M, Hall A, et al. Collagen proportionate area predicts clinical outcomes in patients with alcohol-related liver disease. Aliment Pharmacol Ther. 2020;52(11-12):1728-1738. https://doi.org/10.1111/apt.16111
18. Amernia B, Moosavy SH, Banookh F, Zoghi G. FIB-4, APRI, and AST/ALT ratio compared to FibroScan for the assessment of hepatic fibrosis in patients with non-alcoholic fatty liver disease in Bandar Abbas, Iran. BMC Gastroenterology. 2021 Dec 3;21(1):453. https://doi.org/10.1186/s12876-021-02038-3
19. Ciancio A, Ribaldone DG, Spertino M, Risso A, Ferrarotti D, Caviglia GP, Carucci P, Gaia S, Rolle E, Sacco M, Saracco GM. Who should not Be surveilled for HCC development after successful therapy with DAAS in advanced chronic hepatitis C? Results of a long-term prospective study. Biomedicines. 2023 Jan 9;11(1):166. https://doi.org/10.3390/biomedicines11010166
20. Huang D, Lin T, Wang S, Cheng L, Xie L, Lu Y, Chen M, Zhu L, Shi J. The liver fibrosis index is superior to the APRI and FIB-4 for predicting liver fibrosis in chronic hepatitis B patients in China. BMC Infectious Diseases. 2019 Oct 22;19(1):878. https://doi.org/10.1186/s12879-019-4459-4
21. Tseng TC, Choi J, Nguyen MH, Peng CY, Siakavellas S, Papatheodoridis G, Wang CC, Lim YS, Lai HC, Trinh HN, Wong C. One-year Fibrosis-4 index helps identify minimal HCC risk in non-cirrhotic chronic hepatitis B patients with antiviral treatment. Hepatology International. 2021 Feb;15(1):105-13. https://doi.org/10.1007/s12072-020-10124-z
22. Vallet-Pichard A, Mallet V, Nalpas B, Verkarre V, Nalpas A, Dhalluin-Venier V, et al. FIB-4: an inexpensive and accurate marker of fibrosis in HCV infection. Comparison with liver biopsy and FibroTest. Hepatology. 2007;46(1):32-36. https://doi.org/10.1002/hep.21669
23. Alzubaidi AK, Al-Saadi FA, Fadhil YB. miR-34a and miR-223 as diagnostic biomarkers for the severity of non-alcoholic fatty liver disease. Journal of Genetic Engineering and Biotechnology. 2026 Sep 1;24(3):100784. https://doi.org/10.1016/j.jgeb.2026.100784
24. Esmail VA, Mohammed MO, Al-Nimer MS. Short-term orlistat therapy improves fatty infiltration indices and liver fibrosis scores in patients with non-alcoholic fatty liver disease and metabolic syndrome. Arab Journal of Gastroenterology. 2021 Mar 1;22(1):1-5. https://doi.org/10.1016/j.ajg.2020.12.005
25. Al-Nimer MS. Concomitant determination of haematological indices supported the application of the albumin-bilirubin score in non-malignant liver diseases. World Journal of Hepatology. 2024 Sep 27;16(9):1308. https://doi.org/10.4254/wjh.v16.i9.1308
26. Abbas WAK. Alpha-fetoprotein and high-sensitivity C-reactive protein levels in Iraqi patients with liver cirrhosis. J Popul Ther Clin Pharmacol. 2022;29(3):e11-e16. https://doi.org/10.47750/jptcp.2022.905